Organic & Biomolecular Chemistry

Accepted Manuscript

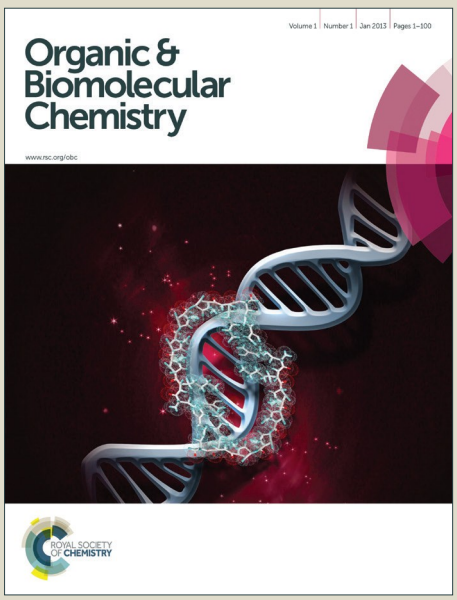

ROYAL SOCIETY OF CHEMISTRY

www.rsc.org/obc

Journal Name

ARTICLE

Steering the Azido-Tetrazole Equilibrium of 4-Azidopyrimidines via Substituent Variation – Implications for Drug Design and Azide-Alkyne Cycloadditions

Received 00th January 20xx,
Accepted 00th January 20xx

DOI: 10.1039/x0xx00000x

www.rsc.org/

A. Thomann,[a] J. Zapp,[b] M. Hutter,[c] M. Empting*,[a] and R. W. Hartmann*,[a,d]

This paper focuses on an interesting constitutional isomerism called azido-tetrazole equilibrium which is observed in azido-substituted *N*-heterocycles. We present a systematic investigation of substituent effects on the isomer ratio within a 2-substituted 4-azidopyrimidine model scaffold. NMR- and IR-spectroscopy as well as X-ray crystallography were employed for thorough analysis and characterization of synthesized derivatives. On the basis of this data, we demonstrate the possibility to steer this valence tautomerism towards the isomer of choice by means of substituent variation. We show that the tetrazole form can act as an efficient disguise for the corresponding azido group masking its well known reactivity in azide-alkyne cycloadditions (ACC). In copper(I)-catalyzed AAC reactions substituent-stabilized tetrazoles displayed a highly decreased or even abolished reactivity whereas the azides and compounds in the equilibrium were directly converted. By use of an acid sensitive derivative, we provide, to our knowledge, the first experimental basis for a possible exploitation of this dynamic isomerism as a pH-dependent azide-protecting motif for selective SPAAC conjugations in aqueous media. Finally, we demonstrate the applicability and efficiency of stabilized tetrazolo[1,5-*c*]pyrimidines for Fragment-Based Drug Design (FBDD) in the field of *quorum sensing* inhibitors.

Introduction

Substituted pyrimidines represent important molecular scaffolds in the fields of biologically active entities,[1] synthetic chemistry,[2] coordination chemistry,[3] and material sciences.[4] The azide functionality, on the other hand, is a highly useful, readily reactive, and easily prepared chemical moiety for bioorthogonal click chemistry,[5] polymer research,[6] and medicinal chemistry.[7]

By the linkage of the azide group to the 2, 4 and/or 6 position of pyrimidines a phenomenon which is referred to as azido-tetrazole equilibrium, can be observed.[8–14] This constitutional isomerism is characterized by a ring closure of the azide with the *ortho*-nitrogen of the pyrimidine core, resulting in the corresponding tetrazole (Scheme 1) and has drawn enormous attention by NMR- and IR-analysts,[8–18] synthetic chemists,[17–25] researchers in drug discovery,[26,27,28] and scientists from the field of computational chemistry.[29–31] Already in 1978, Koennecke *et al.* provided a detailed analysis of substituent-dependent effects on this valence tautomerism

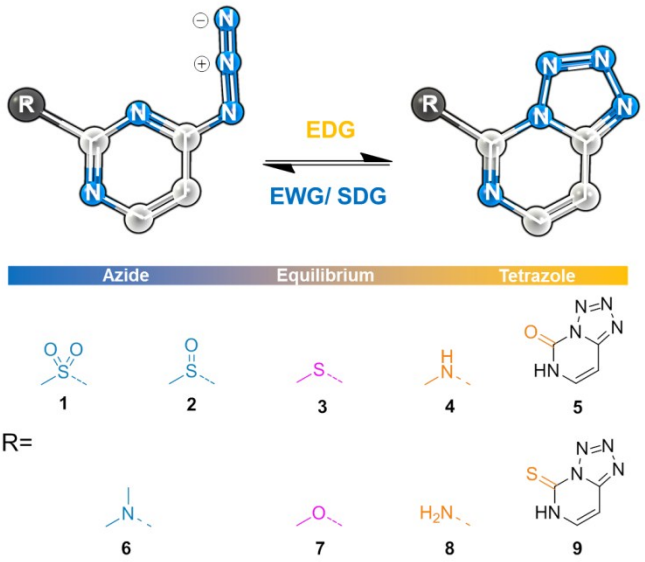

Scheme 1 Depiction of azido-tetrazole equilibrium at 2-substituted 4-azidopyrimidines showing defined substituent effects to steer the equilibrium. Blue substituents fully steer the equilibrium towards the azide tautomer whereas orange groups steer to the tetrazole isomer. Residues which show both isomers are colored accordingly. EDG= electron-donating group, EWG= electron-withdrawing group, SDG= sterically demanding group.

[a] *Helmholtz Institute for Pharmaceutical Research Saarland (HIPS), Department for Drug Design and Optimization (DDOP), Campus C2.3, 66123 Saarbrücken, Germany, E-mail: rolf.hartmann@helmholtz-hzi.de, martin.empting@helmholz-hzi.de.*
[b] *Saarland University, Department of Pharmaceutical Biology, Campus C2.2, 66123 Saarbrücken, Germany.*
[c] *Saarland University, Center for Bioinformatics, Campus E2.1, 66123 Saarbrücken, Germany*
[d] *Saarland University, Department for Pharmaceutical and Medicinal Chemistry, Campus C2.3, 66123 Saarbrücken, Germany*

† Electronic Supplementary Information (ESI) available: Full experimental details, molecular modelling, pK_a determination, LC-MS kinetic analysis, characterization data including ^{1}H-NMR, ^{13}C-NMR, FT-IR , ^{15}N-NMR, X-ray crystallography, HRMS are provided. See DOI: 10.1039/x0xx00000x

and suggested that besides solvent and temperature also electronic as well as steric effects should be considered when investigating the position of the equilibrium.[9] They demonstrated that the electron density at the imino nitrogen ion pair is of particular importance driving the ratio of isomers towards the cyclic tetrazole form. Although their studies were based on a molecular scaffold possessing a different substitution pattern, we concluded that this is the parameter of choice to enforce either of the constitutional states.

In the presented study, we systematically investigated the possibility to steer the equilibrium towards azide or tetrazole isomers by variations of the substituents at the 2 position of 4-azidopyrimidine. To facilitate the establishment of a decent relationship between chemical structure and the position of the equilibrium, we selected different substituents covering a wide range of electronic properties and steric demand. To gather further insight, we conducted density functional calculations including a solvation model using the structures of synthesized derivatives.[32] Such an isomerism should have an impact on reactivity of the azide group.[23] In order to study this effect with our scaffold, we conducted model azide-alkyne cycloaddition (AAC) reactions with selected derivatives resembling both isomers as well as compounds in thermal equilibrium. Finally, such small compounds containing stabilized tetrazoles give rise to fragment-like structures which might be suitable for Fragment-Based Drug Design (FBDD). In a rational approach, we investigated whether these structural features could be exploited for FBDD.

Results and Discussion

Structure Elucidation and Substituent Effects

The effect of substituents on the azido-tetrazole equilibrium of 4-azidopyrimidines has been described for a small subset of a heterogeneously substituted series.[8,13,33] In contrast to more intensely studied 2-azidopyrimidines[10,11,14] this molecular scaffold displays only one possible cyclization geometry and, hence, just one tetrazole isomer. Notably, derivatives of 4-substituted pyrimidines have recently moved into the focus of our research[34] emphasizing their relevance as starting points for the design and synthesis of biologically active entities. The occurrence of the described constitutional isomerism in azido-pyrimidines added another level of structural complexity and variability to the compounds which we wanted to investigate in more detail. To the best of our knowledge, no rational approach to steer the equilibrium in this system towards desired connectivity and, hence, activity by substituent variation has been described to date. Therefore, we chose nine functional groups, different in electronic and steric properties, as substituents in the 2-position to study the effect on the equilibrium (Scheme 1 and 2).

As shown before, the equilibrium can be directly monitored by ^{1}H-NMR and ^{15}N-NMR.[8–10,13,15–18,35,36] According to ^{1}H-NMR spectral data the doublets for the two protons at C-5 and C-6 of the pyrimidine ring are distant to each other for the azide

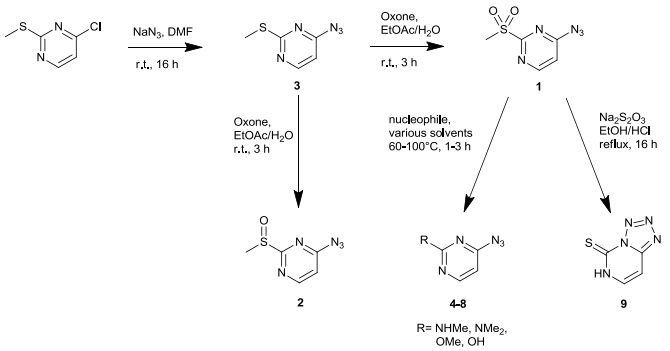

Scheme 2 Synthesis of compounds **1**-**9**.

Table 1 Substitution pattern of compounds **1**-**9** and the observed effect on the equilibrium determined by ^{1}H-NMR in DMSO, IR and X-ray crystallography.

Cmpd	Group	Effect[a]	^{1}H-NMR[b]	IR	X-Ray[b]
1	SO_2Me	EWG/ SDG	A	Strong Azide	-
2	SOMe	EWG	K_T = 33.3	Strong Azide	-
3	SMe	EDG	K_T = 0.20	Intermediate Azide	T
4	NHMe	EDG	T	No Azide	T
5	Carbonyl	EDG	T	Weak Azide	T
6	NMe_2	EDG/ SDG	K_T = 10.0	Strong Azide	-
7	OMe	EDG	K_T = 1.5	Intermediate Azide	-
8	NH_2	EDG	T	No Azide	-
9	Thionyl	EDG	T	No Azide	-

[a] EDG= electron-donating group, EWG= electron-withdrawing group, SDG= sterically demanding group; [b] A= azide, T= tetrazole, K_T = equilibrium constant[11]

(Δppm = 1.0-1.9) and are closer and downfield shifted for the tetrazole-form (Δppm = 0.2-0.8) (Figure 1A).[8,10,12]

In case of compound **1**, bearing a sulfomethyl-group in 2-position, ^{1}H- and ^{15}N-NMR spectra provided a signal set of only one isomer with chemical shifts resembling the monocyclic variant (Figure 1A, Electronic supplementary information (ESI) section II.e). This finding was supported by IR data, as we observed the characteristic absorption band at 2100 cm^{-1} (Figure 1B).[37] Hence, under the conditions used (ambient temperature, DMSO as solvent) only the azide form of compound **1** is detectable.

The complete absence of the tetrazole valence tautomer is quite notable, as this cyclic isomer is considered to be the favored low temperature structure in case of pyridine, pyrazine, and pyrimidine cores.[38] Both steric as well as electronic effects induced by the bulky, electron-withdrawing sulfomethyl moiety might be responsible for this result. To further investigate this, we synthesized compound **2** bearing a sulfoxide, which possesses a lower steric demand but has almost equal electron-withdrawing properties (Hammett constants are $\sigma_{m,SOMe}$ = 0.52 and $\sigma_{m,SO2Me}$ = 0.60).[39] Interestingly, we observed a signal subset of very low intensity

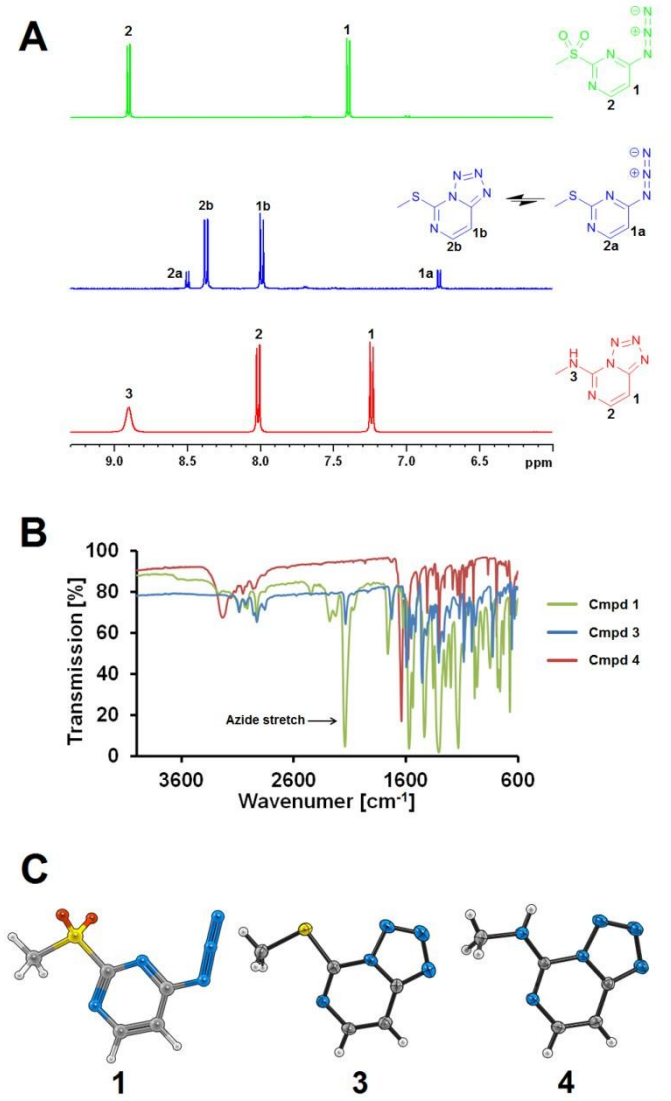

Figure 1 Analytical data of compounds **1** (green), **3** (blue) and **4** (red) allowing for the determination of azide and tetrazole isomers. ^{1}H-NMR (A), IR (B), X-ray crystallography (**3** and **4**) and modeling of compound **1** (energy optimized using MM2 semi-empirical method) (C). ^{1}H-NMR chemical shifts for protons at C5 and C6 of tetrazole tautomers are significantly closer to each other (**3**: Δppm= 0.4, **4**: Δppm= 0.8) than respective signals for azide isomers (**1**: Δppm= 1.5, **3**: Δppm= 1.7) (A). ^{15}N-NMR chemical shifts (B) and azide-band appearance at ~2100 cm^{-1} in IR (B) support the structural proposals (**4** only tetrazole, **3** both isomers, **1** only azide) shown in Table 1. In the crystal form only tetrazole tautomers were observed as determined by X-ray crystallography for compounds **3** and **4** (C).

within the ^{1}H-NMR-spectum belonging to the tetrazole form, while the main isomer for **2** was showing chemical shifts of the azide (Table 1). This finding suggests that bulky substituents in 2 position may favor the azide. The sulfomethyl group of **1** might cause steric clashes upon formation of the tetrazole which impair the degree of rotational freedom at the substituent site. This penalty would be less pronounced in case of sulfoxide **2** providing a possible explanation for the presence of the tetrazole at detectable levels.

To investigate the effect of electron-donating groups (EDG) we introduced thiomethyl (**3**) and methoxy (**7**) substituents. Interestingly, both compounds were in the equilibrium state whereas the thiomethyl derivative showed more tetrazole character (Figure 1A, Table 1, ESI section II.a). Comparing the Hammett constants[39] of both groups, the methoxy-substituent (σ_m = 0.15) is less electron donating compared to its thio isostere (σ_m = 0.12). These results are consistent with the hypothesis that EWGs in 2-position favor the azide over the tetrazole (Table 1). This trend can also be witnessed by comparing the IR-spectra as compounds **3** and **7** show weaker azide bands than **1** (Figure 1B, ESI section II.g). In addition to NMR and IR, we performed X-ray structure analysis with selected compounds that were readily crystallizable (Table 1). However, even for compound **3** only the tetrazole form was observed in the elucidated structure (Figure 1C). This might be a result of the crystallization procedure favoring those isomers which pack more densely. Notably, no crystals were obtained for compounds showing the most pronounced azide character (**1**, **2**, **6**, and **7**).

With the aim to further investigate the influence of EDGs, we decorated the 2-position with a series of substituents possessing ascending electron-donating properties by introduction of an amine (**8**), a methylamine (**4**) and a dimethylamine group (**6**).[39] Again we collected ^{1}H-NMR and IR data for these compounds and, additionally, elucidated the structure of compound **4** by ^{15}N-NMR and X-ray crystallography. We found the equilibrium to be fully shifted towards the tetrazole in case of compound **4** (Figure 1, Table 1, ESI section II.e) and **8** (Table 1). Interestingly, dimethyl derivative **6** was found to exist mainly in the azido state as indicated by ^{1}H-NMR and IR analysis (Table 1, ESI section II.a,g) although it is the group with the strongest electron-donating properties within this subset of compounds (**4**, **6**, **8**). As hypothesized before (in the case of compound **1** and **2**, *vide supra*), the space demanding properties of the two methyl groups of compound **6** may force the equilibrium towards the azide. We found the proton at the amine within the crystal structure of closely related tetrazole **4** to be in proximity to the neighboring nitrogen of the tetrazole-ring (Figure 1C). Upon replacing this proton by a methyl group *in silico* (yielding the tetrazolo isomer of **6**), intramolecular steric clashes occur between the newly introduced group and the tetrazole nitrogen (ESI section I.d). These results might explain the shift of the thermal equilibrium towards the azide form underlining the impact of steric factors in the likelihood of the cyclic valence tautomer. The involvement of an intramolecular hydrogen bond for stabilization of the tetrazole over the azide-isomer in **4** was ruled out by monitoring of the N-H shift in $CDCl_3$ under DMSO titration as described before (ESI section II.b).[40]

As we were also interested in the thiol and hydroxy derivatives, we synthesized compounds **5** and **9**. However, as reported before,[41] these structures could not be obtained as the free hydroxy or thiol compounds but "trapped" in urea-like tautomers. For both compounds the equilibrium was fully shifted towards the tetrazole as indicated by ^{1}H-NMR (Table 1) and X-ray crystallography (ESI section I.b). Previous studies on the structure of **5** were based on its UV spectrum and the authors Fox *et al.* could, therefore, only speculate that it might be the tetrazole derivative.[41] As the structures of **5** and **9** are similar to 2-hydroxypyrimidine, which was reported to be NH acidic (pK_a= 2.9),[42] we hypothesized that **5** and **9** could also be acids.

Table 2 Calculated differences in solvation energy obtained by the COSMO solvent model. Library compounds **1**-**9** were energetically minimized at the B3LYP/aug-cc-pVDZ level of theory. Units are given in kcal/mol.

Cmpd	Water		DMSO		Chloroform	
	A	T	A	T	A	T
1	-2.48	0	-2.14	0.0	-	-
2	0	-1.04	0	-1.02	0	-0.88
3	0	-5.14	0	-5.88	0	-4.93
7	0	-4.16	0	-4.14	0	-3.70
6	0	-2.96	0	-3.26	-	-
4	0	-2.96	0	-3.62	-	-
8	0	-5.99	0	-6.77	-	-
5	0	-8.57	0	-10.48	-	-
9	0	-10.27	0	-8.68	-	-

A= Azide, T=Tetrazole

To check this hypothesis, we determined pK_a values for compound **5** and **9**. Interestingly, **9** turned out to be even as acidic as acetic acid with a pK_a of 4.6. Compound **5** (pK_a = 6.8) is two orders of magnitude less acidic than **9**. Furthermore, we concluded from these findings that the polarization of the hydrogen at N6 could lead to an increased electron density in the ring system, resulting in the preference for the tetrazole.

In summary, we have shown that EDGs favor the tetrazole while electron-withdrawing-groups (EWGs) shift the equilibrium towards the azide (Scheme 1). However, sterically demanding substituents may suppress formation of the cyclic isomer even with strong EDGs being present.

To further investigate the influence of substituents in 2-position on the electronic properties and, hence, the stability of the corresponding constitutional isomers, we performed hybrid density functional theory (DFT) calculations including a continuum solvation model. Previous molecular modeling experiments in this field applied gas-phase DFT calculations to evaluate azido-pyridines and its tetrazolo analogues *in silico*.[29–31] As mentioned above, solvent effects may significantly contribute to the state of the equilibrium.[8,10] In the present study, we used the COnductor-like Screening MOdel (COSMO) solvation methodology[32] as implemented in NWChem (version 6.1) to predict the contributions of water, DMSO and $CHCl_3$. This procedure provides a high numerical efficiency facilitating fast calculations while retaining sufficient accuracy especially in solvents with high permittivity (e.g. water).[43] For energy optimization we chose B3LYP/aug-cc-pVDZ level of theory.

For the accurate computation of similar isomerization energies *in vacuo*, Grimme *et al*. showed that coupled-cluster methods are most reliable and pointed out some flaws of the popular B3LYP density functional for the determination of kinetic and thermodynamic energy terms.[44] In particular the transformation of π into σ bonds shows substantial errors.[45] Likewise, Grimme and co-workers found that only triple-ζ basis sets such as the here applied aug-cc-pvdz basis set are necessary for obtaining precise results. On the other hand, the mentioned drawbacks of the B3LYP functional do not affect the prediction of molecular structures that are required for subsequent single-point energy computations, using for example other density functionals, higher-level methods, or solvent models.

As a result, our computations suggested that the tetrazole form is mostly energetically favored except for derivative **1** (Table 2). Hence, the absolute position of the equilibrium differed from that observed in our NMR and IR experiments.

We attribute the systematic over-estimation of the stability of the tetrazole form to the fact that hydrogen-bonding and any other directional interactions with the solvent are not considered because the solvent is treated as continuum, whereby its dielectric constant is the decisive parameter. Thus, these kind of interactions, which are likely to shift the tautomeric equilibrium, are beyond the scope of conventional density functional methods and continuum solvation models.

Nevertheless, several qualitative aspects of the constitutional isomerism could be reproduced *in silico* quite well. For example, our experimental data (ESI section II.b) and the literature suggested,[8,10] that less polar solvents favor the azide form in contrast to polar ones. In case of compound **1** the predictions perfectly matched the experimental results with the azide being the predominant species. Additionally, for **5** and **9** a rather high preference for the cyclic form was predicted with an energy difference of -8.57 kcal*mol^{-1} and -10.27 kcal*mol^{-1}, respectively. Hence, the calculations suggest that according to the Boltzmann distribution only one ppm or less of the compounds exists in the azide form at room temperature.[46] In accordance with that, no signals for the azide-isomer have been observed for **5** and **9** by NMR characterization (*vide supra*). For compounds **3** and **7** we observed both isomers in our experiments. The former favors the tetrazole and the latter the azide form under the conditions used (Table 1). Our computational results, however, suggest that both forms preferably adopt the cyclic constitution. Nevertheless, the calculated energy difference for thiomethyl **3** was higher than for its methoxy congener **7** which describes the general trend correctly.

In case of amines **6**, **4**, and **8**, all derivatives were predicted to favor the tetrazole form. While primary amine **8** displayed the strongest preference for the cyclic isomer in this subset, the secondary (**4**) and tertiary (**6**) variants both yielded similar values regarding calculated energy difference. Experimentally, we determined a ten-fold excess of azide form for the latter while the secondary amine was confirmed to be a tetrazole as predicted. We assume that the observed discrepancy between computational and experimental results is caused by a steric effect of the bulky dimethyl functionality attenuating cyclisation propensity which is not properly accounted for by the DFT method.

For compound **2** only a small difference between the azide and the tetrazole isomer of about 1 kcal*mol^{-1} was predicted indicating that both forms are suggested to exists in a near equal ratio with a slight preference for the cyclic one. Our experiments, however, clearly show a strong shift of the equilibrium towards the azide. Nevertheless, in comparison with the other compounds predicted to be tetrazoles (**3** - **9**) sulfoxide **2** displays the lowest preference for the cyclic isomer. Hence, although the overall outcome of our

calculations is biased towards the tetrazole, the general trend is described quite well.

Implications for copper-catalyzed azide-alkyne cycloaddition (CuAAC)

The copper-catalyzed azide-alkyne cycloaddition (CuAAC) is the method of choice for the synthesis of 1,4-disubstituted 1,2,3-triazoles and is known to proceed under mild conditions (e.g. in water at ambient temperature).[47] Since its first appearance in the literature in 2002,[48] it has had a huge impact in all fields of synthetic chemistry. Notably, a variety of applications in drug design and medicinal chemistry including fast compound library generation, bioconjugation, or bioisosteric replacements has been developed in the last decade.

The effects of the constitutional isomerism on triazole formation was investigated for pyridine compounds,[17,23,25] quinazoline derivatives,[49] as well as azidopurines.[18,24,35,36,50] Furthermore, in a computational study the effect of copper(I) species (in this case CuCl) on the azido-tetrazole equilibrium in pyridine and imidazole test systems was investigated.[51] Depending on the scaffold, the coordination of the transition metal can have a stabilizing effect on the tetrazole isomer (pyridine) but also the azide form (imidazole). Hence, a possible shift of the equilibrium under CuAAC conditions in the pyrimidine system described herein cannot be excluded.

These results demonstrated that tetrazole formation has a detrimental effect on the yield of this reaction type. For pyrimidines, especially 2-azidopyrimidines, the impact of the tautomerization on CuACC has not been investigated, yet. Only few reports about the transformation of 2-azidopyrimidines[19] and 4-azidopyrimidines[20–22] into the corresponding triazoles have been published to date. However, in the aforementioned studies usage of Huisgen conditions (high temperature, no catalyst) resulting in a mixture of 1,4- and 1,5-disubstituted regioisomers (for terminal alkynes) or trisubstituted triazoles (for internal alkynes) is described. To address the impact of heat on the equilibrium, we run a temperature gradient ^{1}H-NMR experiment and observed a shift from tetrazole to the azide species for compound **3** (ESI section II.f) upon raising temperature. This is in accordance with the literature as the azide is described to be the high-temperature species.[9] Hence, Huisgen conditions intrinsically favor the open form directly facilitating thermal AAC. As ambient temperature is applicable for routine CuAAC reactions, we expected that the impact of the tautomerism and the state of the equilibrium would be more pronounced under these mild conditions. It has been reported that electronic as well as steric features of substituents at the azide group may influence the reaction rate of the CuAAC reaction.[52] We were curious how our "stabilized" azide (compound **1**), the equilibrium state (compound **3**) and the "stabilized" tetrazole (compounds **4** and **5**) behave in the click reaction. Therefore, we used phenylacetylene, $CuSO_4$*$5H_2O$, and sodium ascorbate in *tert*BuOH:water (1:1) as

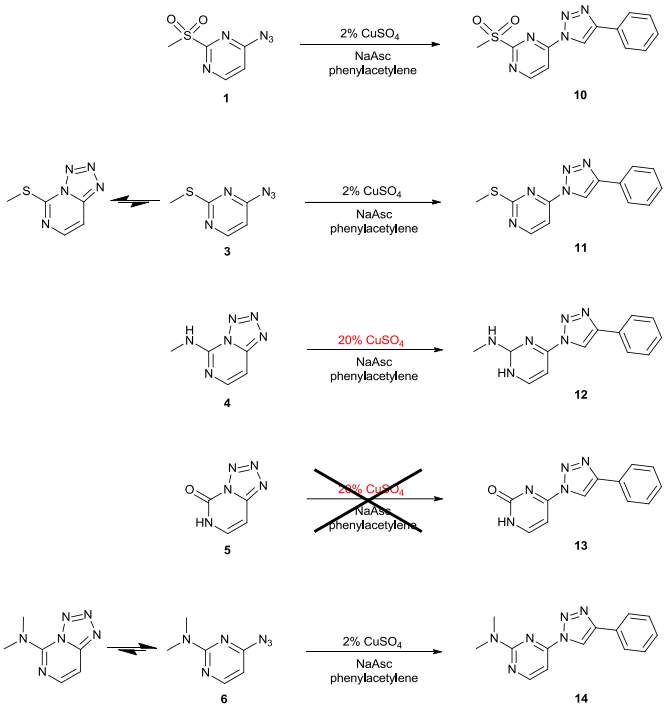

Scheme 3. Model CuACC reaction for the synthesis of triazoles **10-14**, employing phenylacetylene, $CuSO_4$ and sodium ascorbate (NaAsc). Compounds **1**, **3** and **6** readily undergo the reaction while compound **4** only reacts upon high catalyst load. Compound **5** remained "unclickable" under the applied conditions.

Table 3 Isolated yields of model CuACC reactions for the synthesis of triazoles **10-15** employing phenylacetylene, $CuSO_4$ and sodium ascorbate. Compounds **1**, **3** and **6** readily undergo the reaction while compound **4** only reacts upon high catalyst load. Compound **5** remained "unclickable" under the applied conditions.

Compound	2%[a]	20%[a]
1	55%	-
3	81%	-
4	0%	51%
5	0%	0%
6	68%	-

[a] mol% of $CuSO_4$·$5H_2O$

a model system and monitored the reactions via LC-MS analysis.

Sulfone-containing compound **1**, although being fully shifted towards the azide, gave lower isolated yield than its thiomethyl analogue **3**. A possible explanation might be the different electronic properties of both groups which could influence azide reactivity (*vide supra*). Whether the azide group of is more activated or not, it seems that as long as there is the open species present in a significant amount the CuAAC reaction proceeds (Scheme 3, Table 3).

To corroborate these results, we employed **6** in the same reaction. Analogous to **1** and **3**, compound **6**, mainly existing as azide, was directly convertible towards triazole product **14** (Table 3, Scheme 3, ESI section I.a) using 2 % copper(I) catalyst. For the stabilized tetrazoles **4** and **5** no product was found in our LC-MS analysis. Hence, tetrazole formation suppressed the CuAAC reaction under the used conditions. To increase

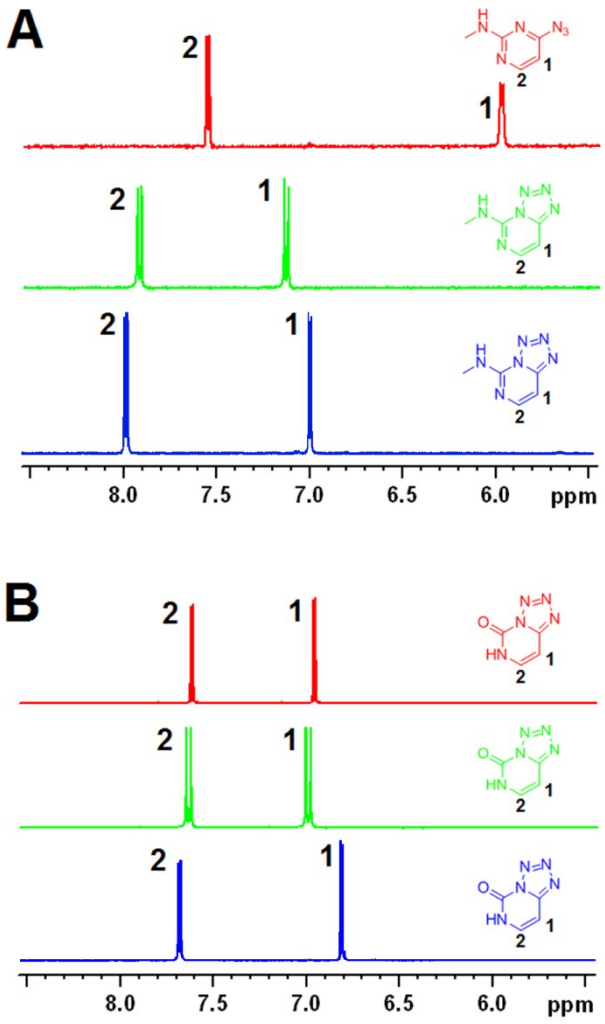

Figure 2 pH dependency of the azido-tetrazole equilibrium of compounds **4** (A, green spectrum D_2O, red spectrum D_2O + TFA, blue spectrum D_2O + NaOH) and **5** (B, green spectrum D_2O, red spectrum D_2O + TFA, blue spectrum: D_2O + NaOH) monitored by ^{1}H-NMR. Results indicate a tetrazole ring opening under acidic treatment of **4** whereas **5** remains as the tetrazole isomer.

reaction speed and yield, we increased the amount of copper(I) catalyst by the factor of ten (Scheme 3 , Table 3). Indeed, we were able to obtain the triazole compound **12** using aminomethyl **4** as educt. Interestingly, derivative **5** did not react even under these conditions indicating that tetrazole formation successfully abolished CuAAC reactivity of this compound (Scheme 3, Table 3). Nevertheless, access to the carbonyl-derivative decorated with a triazole in 4-position could be gained through treatment of **10** with sodium hydroxide in a dioxane/water mixture to transform the sulfomethyl group into the mentioned carbonyl compound.

Implications for Strain-Promoted Azide-Alkyne Cycloaddition (SPAAC)

Strain-promoted azide-alkyne cycloaddition has drawn enormous attention by the biological and chemical community because of its ability to be directly used in cellular systems[53] without the need of cytotoxic copper or ruthenium catalysts. It was described that acidic conditions lead to a ring opening of the tetrazole shifting the equilibrium towards the azide.[9,12] To

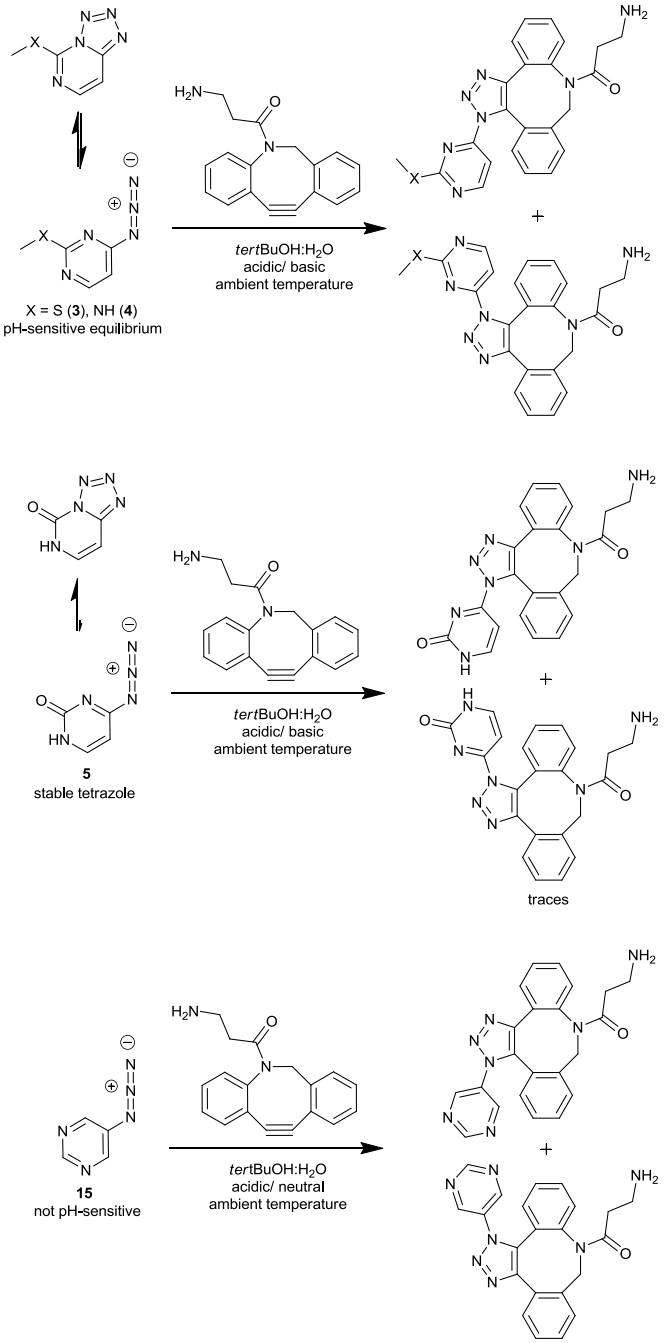

Scheme 4 SPAAC of pH-sensitive 4-azidopyrimidines **3**, **4**, **5** and pH-non-sensitive 5-azidopyrimidine (**15**) and dibenzocyclooctyne-amine under varying pH environments in aqueous media.

investigate the effect of acidic, basic, and neutral conditions on our stabilized tetrazoles we chose compound **4** and **5** to determine the equilibrium under the influence of TFA and sodium hydroxide. Under neutral and basic conditions, the compound remained in its tetrazole form. Noteworthy, under harsh basic conditions (1 M NaOH) an additional minor signal set occurred that was due to compound degradation (ESI section II.c). As expected, signals of **4** shifted under acidic treatment indicating a ring opening and formation of the azide. This was confirmed by the appearance of the characteristic band in the IR spectrum for the hydrochloric salt of **4** (Figure 2A, ESI section II.g).

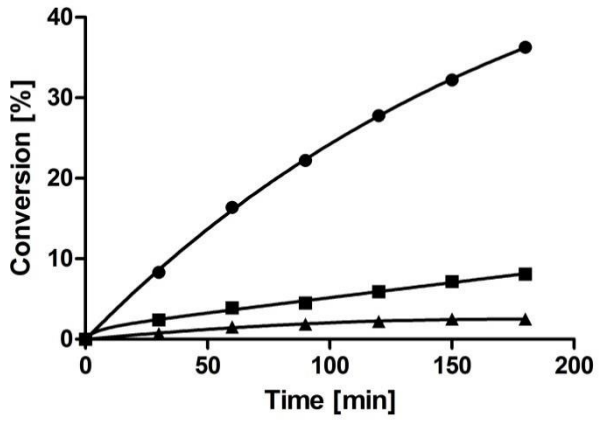

Figure 3 Kinetic analysis of the SPAAC of compound **4** and dibenzocyclooctyne-amine at pH 1.5 (●), 2.5 (▪) and 4.1 (▲) at room temperature. Conversion was monitored by LC-UV_{254} and products were identified by mass spectrometry.

Interestingly, **5** was not convertible to the azide through TFA treatment. Under neutral and acidic conditions only NMR signals assigned to the tetrazole form were detected (Figure 2B).

Motivated by these results, we used compounds **4**, **5**, and **3** in a pH-dependent SPAAC reaction with dibenzocyclooctyne-amine to see whether the pH sensitivity of the equilibrium effects reactivity (Scheme 4). As expected, **3** reacted under all conditions with the SPAAC reagent but with a significantly higher reaction rate in the acidic environment (Table 4, ESI section I.h).

As suggested by the ^{1}H-NMR results compound **4** readily reacted in 0.1 M HCl or 0.2% TFA but was almost unreactive under neutral or basic conditions (0.1 M NaOH) as indicated by LC-MS experiments. Moreover, stronger acidic conditions (0.1 M HCl) resulted in a higher reaction rate compared to the less acidic one (0.2% TFA), suggesting a clear pH dependency of the reactivity (ESI Section I.h). To confirm this hypothesis, we monitored the reaction of compound **4** and dibenzocyclooctyne-amine under different acidic pH conditions (Figure 3, Table 4). These results clearly demonstrate the pH-dependent acceleration of the reaction when shifting the milieu towards higher acidity. Finally, compound **5** was only able to undergo SPAAC in traces in the acidic or neutral environment but remained unreacted under basic conditions (ESI section I.h). However, differences in conversion could potentially also arise from a protonation leading to altered reactivity of the azide-group. To evaluate whether low pH has a direct effect on azide reactivity we synthesized 5-azidopyrimidine (**15**, Scheme 4, ESI section I.a). Compound **15** is not able to form a tetrazole and was used in a SPAAC reaction with dibenzylcyclooctyne-amine at pH 1.4 and pH 7.0 (Table 4, ESI section I.i). For these two environments no difference in product formation over time and total conversion after 3 hours was found. Hence, a direct influence of acidic pH on azide reactivity, e.g. via protonation of the pyrimidine core, can be excluded in this case. Moreover, these results indicate that the improved reactivity of **4** at low pH mainly depends on tetrazole ring opening. These results are in good accordance

Table 4. LC-MS conversions of model pH dependent SPAAC reactions employing dibenzylcyclooctyneamine with **3**, **4** and **5** after 1.5 hours of reaction time in 0.1 M HCl, 0.2% TFA and 0.1 M NaOH in *tert*BuOH:water (1:1). **4** showed increased click-reactivity upon decreasing pH whereas pure azide **15** was equally reactive at pH 1.4 and 7.0 after 3 hours at ambient temperature.

Cmpd	HCl_{aq} 0.1M	TFA_{aq} 0.2%	$NaOH_{aq}$ 0.1M	pH 7.0[a]	pH 4.1[b]	pH 2.5[c]	pH 1.4[d]
3	32%	28%	4%	-	-	-	-
4	51%	23%	1%	-	3%	8%	36%
5	<1%	<1%	<1%	-	-	-	-
15	-	-	-	77%	-	-	77%

[a]aqueous phosphate buffer + *tert*BuOH (1:1), [b]aqueous acetate buffer + *tert*BuOH (1:1), [c]0.01 M HCl $_{aq}$ (*tert*BuOH:H_2O, 1:1), [d]0.1 M HCl_{aq} (*tert*BuOH:H_2O, 1:1), Conversions were monitored by LC-UV_{254}-MS

with our data on the "unclickability" of compound **5** in CuAAC reactions (Table 3). More importantly, our results gathered for compound **4** hint at the possibility to exploit this tautomerism effect as a pH-dependent atom-economic protection method for the azide group. This would allow to regioselectively address different azides within the same molecule simply by reversibly capping one of them as a tetrazole via simple pH adjustments. In light of the fact that CuAAC reactions are routinely carried out in the presence of a tertiary amino base (e.g. Hünig's base)[54] a regioselective sequence of CuAAC and SPAAC might be achieved.

Implications for Fragment-Based Drug Design (FBDD)

FBDD has attracted huge attention in the past decade.[55] The advantages of fragments lie in their low molecular weight and the possibility to generate high structural diversity by use of rather small libraries. In general, all ligands need to overcome the translational and rotational rigid body entropy barrier[56] to attractively interact with a protein target. As fragment-like compounds possess only a few pharmacophore features due to their small size, they are supposed to display near optimal binding modes to be able to overcompensate the entropy term of the freely diffusing solute. As a result, fragment-sized binders usually display high ligand efficiencies, a metric used to evaluate inhibitors with regard to their molecular weight.[57] This, in combination with favorable physicochemical properties, renders such fragment hits as ideal starting points for further drug development.[58] Several molecular parameters have been defined as guideposts for straightforward design of fragment libraries and are usually referred to as the Astex `rule of 3´.[59]

With these concepts in mind, we hypothesized that our substituent-stabilized tetrazolopyrimidines might be suitable candidates for FBDD. Noteworthy, such molecular scaffolds can be found as substructures in pharmaceutically relevant entities[26,28] and share some similarity with purine nucleobases present in many biologically active compounds. Coenzyme A (CoA), for example, is a molecule which incorporates an adenosyl moiety and is involved in many cellular processes.[60] It is employed by nature as an acyl carrier to provide thioester-activated substrates for a large variety of enzymes. One acetylase that is in the focus of our research and uses such

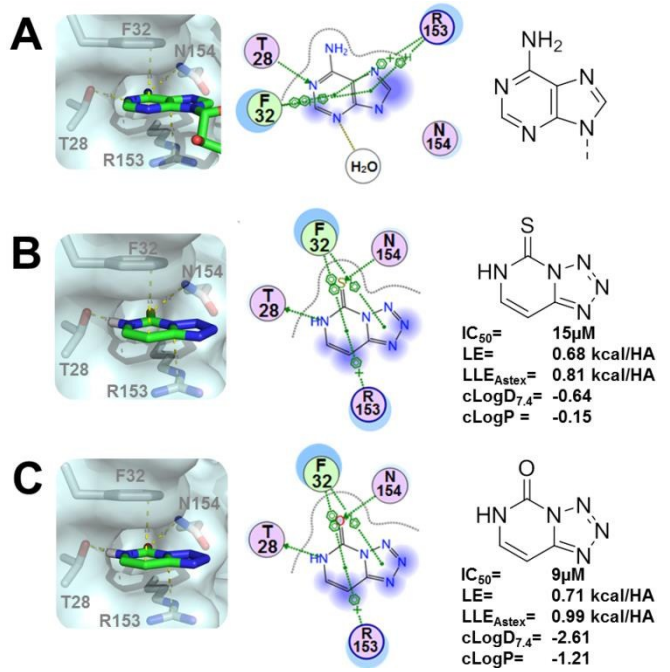

Figure 4. $cLogD_{7,4}$, cLogP, IC_{50}s, ligand efficiency indices and predicted interactions of **9** (B) and **5** (C) in comparison with the natural substrate anthraniloyl-CoA (A) in the adenosyl-pocket of PqsD (PDB-ID: 3H77). Both LE[63] and LLE_{Astex} were calculated based on IC_{50}s. HA= Heavy Atom Count.

CoA-linked structures is called PqsD.[61,62] It is a bacterial signal molecule synthase found in the opportunistic human pathogen *Pseudomonas aeruginosa*. PqsD is essential for the production of the so-called Pseudomonas Quinolone Signal (PQS).[62] This autoinducer is the eponymous molecule driving the PQS *quorum sensing* (QS) system – a cell-to-cell communication apparatus regulating pathogenicity-determining factors of *P. aeruginosa*. In this regard, we have shown before that blocking PqsD by small molecule inhibitors leads to reduction of biofilm formation rendering this enzyme a potential novel target for anti-infective agents.[61] Both substrates of this enzyme, anthraniloyl-CoA and malonyl-CoA, carry the adenosyl moiety.[62] Guided by the above-mentioned rational that our fragments have a high degree of similarity towards this residue (Figure 4, Scheme 1) we assumed that these compounds may bind to PqsD and could potentially inhibit the enzyme reaction. Indeed, two of our tetrazole fragments (**5** and **9**) displayed IC_{50} values in the lower micromolar range resulting in high ligand efficiencies (Figure 4B and 4C). The optimal starting point for FBDD is a LE score of at least 0.3[58,64] whereas our fragments possess LE's which are at least two-fold higher than this proposed mark (Figure 4B and 4C).

Comparison of the IC_{50}s of **5** and **9** (Figure 4B and 4C) revealed the carbonyl to be slightly advantageous for activity. Having in mind our working hypothesis that the fragments might occupy the adenosyl site at the surface of PqsD, we modeled the fragments into that pocket using the X-ray cocrystal structure of PqsD and anthraniloyl-CoA (PDB-ID: 3H77).

The modeling results suggest that the carbonyl and thionyl moieties of **5** and **9** form a hydrogen bond with N154 (Figure 4). This interaction might be weaker for the thionyl pendant **9** which is known to be a less potent hydrogen bond acceptor.[65]

Additionally, the protonated nitrogen of the pyrimidine core may act as a hydrogenbond donor to T28 (Figure 4B and 4C). With regard to acidic character of **5** and **9** it is also plausible that the compounds are deprotonated at the nitrogen in 6-postion and, hence, could interact as hydrogenbond acceptors for the side chain of T28 like the adenosyl moiety in the crystal structure. Moreover, the electron-enriched tetrazolopyrimidines could form stronger pi interactions with R153 and F32. To derive further SAR (structure-activity relationship) information regarding the structural prerequisites for activity we also tested hypoxanthine and adenine for PqsD inhibition. Although being quite similar to **5** and **9**, hypoxanthine showed only 9% enzyme inhibition at 50 µM while adenine was inactive at this concentration (see ESI section I.g). These findings underline the value of **5** and **9** as fragment-inhibitors of PqsD, but also shed light on the tight SAR at the tetrazolo substructure which demonstrates higher potency than the tested imidazolo congeners.

It is well known that during a drug optimization campaign compounds tend to become larger and more lipophilic.[66] Therefore, it is of great importance to start from a core molecule with low cLogP and $cLogD_{7,4}$ values. As lipophilicity is of great importance for solubility and passive diffusion over the plasma cellular membrane a new metric has been introduced: ligand lipophilicity efficiency (LLE).[67] This metric evaluates compounds not only on their activity and molecular weight but also on their lipophilicity. Notably, our fragments perform even better with regard to this novel efficiency index than in the traditional ligand efficiency rating (Figure 4B and 4C).

Accordingly, both metrics suggest that these fragment inhibitors could be ideal starting points for further FBDD efforts towards novel drug-like inhibitors of PqsD and, hence, potential anti-biofilm agents.

Conclusions

In summary, the data presented in this paper provides the basis for a rational approach towards steering the azido-tetrazole equilibrium within 4-azidopyrimidines. By choice of the substituent in 2-position either the azide or the tetrazole isomer can be efficiently stabilized. These findings provided insights into substituent effects like the electronic and steric parameters influencing this phenomenon. This information was used to evaluate azide-based compounds which are readily "clickable", "poorly clickable" and "unclickable" in a model copper-catalyzed click reaction. In additional experiments, we demonstrated a pH-dependent protecting group characteristic of the acid-sensitive tetrazole in SPAAC reactions. These results may motivate the application of azidopyrimidine moieties for the regio-control of multi-step AAC reactions. Such a strategy could be exploited for the facile generation of heterovalent bioconjugates or may pave the way towards pH-selective labeling in acidic cellular environments like lysosomes[68] as well as cancerous[69] or inflammatory tissue[70] via bioorthogonal click chemistry.

Despite the limitations of the applied solvent model in our DFT calculations general trends could be described quite well and experimental data for further optimization of these models towards better predictive power were provided. Finally, the analytical results were used for a FBDD approach towards inhibitors of PqsD, a reported anti-biofilm target. The usefulness of these fragments as potential analogues of adenosyl motifs has been demonstrated and may lead to further fragment-based drug development campaigns.

Acknowledgements

We like to thank Michael Hoffmann for recording HRMS spectra, Giuseppe Allegretta for the determination of the pk_a of compounds **5** and **9**, and Volker Huch for recording the X-ray crystalstructures of compounds **3**, **4** and **5**. This project was funded by BMBF through grant 1616038B

References

1 a) S. Fujii, T. Kobayashi, A. Nakatsu, H. Miyazawa and H. Kagechika, *Chem. Pharm. Bull.*, 2014, **62**, 700–708; b) A. McCluskey, P. A. Keller, J. Morgan and J. Garner, *Org. Biomol. Chem.*, 2003, **1**, 3353; c) Mohite, P., B., Pandhare, R., B. and S. G. Khanage, *Biointerface Res. Appl. Chem.*, 2012; d) T. Nagata, K. Masuda, S. Maeno and I. Miura, *Pest management science*, 2004, **60**, 399–407;

2 a) D. Meyer, M. A. Taige, A. Zeller, K. Hohlfeld, S. Ahrens and T. Strassner, *Organometallics*, 2009, **28**, 2142–2149; b) G.-L. Wu, S.-L. Cao, J. Chen and Z. Chen, *Eur. J. Org. Chem.*, 2012, **2012**, 6777–6784; c) Schuchardt, Jonathan, L., *Patent WO 02/098931 A1*, 2002;

3 a) T. D. Nixon, A. J. Gamble, R. J. Thatcher, A. C. Whitwood and J. M. Lynam, *Inorg. Chim. Acta*, 2012, **380**, 252–260; b) S. Roy, T. N. Mandal, A. K. Barik, S. Pal, S. Gupta, A. Hazra, R. J. Butcher, A. D. Hunter, M. Zeller and S. K. Kar, *Polyhedron*, 2007, **26**, 2603–2611; c) A. Rodríguez, A. Sousa-Pedrares, J. A. García-Vázquez, J. Romero and A. Sousa, *Polyhedron*, 2009, **28**, 2240–2248;

4 a) S. S. Gunathilake, H. D. Magurudeniya, P. Huang, H. Nguyen, E. A. Rainbolt, M. C. Stefan and M. C. Biewer, *Polym. Chem.*, 2013, **4**, 5216; b) A. Slaczka and J. Lubczak, *Polimery*, 2010, **55**, 681–684; c) A. Gallego, O. Castillo, C. J. Gómez-García, F. Zamora and S. Delgado, *Inorg. Chem.*, 2012, **51**, 718–727;

5 a) C. Besanceney-Webler, H. Jiang, T. Zheng, L. Feng, Soriano del Amo, David, W. Wang, L. M. Klivansky, F. L. Marlow, Y. Liu and P. Wu, *Angew. Chem. Int. Ed.*, 2011, **50**, 8051–8056; b) P. Shieh, M. S. Siegrist, A. J. Cullen and C. R. Bertozzi, *Proc. Natl. Acad. Sci. U. S. A.*, 2014, **111**, 5456–5461;

6 a) L. Billiet, X. K. Hillewaere and Du Prez, Filip E., *Eur. Polym. J.*, 2012, **48**, 2085–2096; b) S. K. Reshmi, K. P. Vijayalakshmi, D. Thomas, E. Arunan and Reghunadhan Nair, C. P., *Propellants, Explos., Pyrotech.*, 2013, **38**, 525–532; c) H.-k. Li, J.-z. Sun, A.-j. Qin and B. Z. Tang, *Chin. J. Polym. Sci. (Chinese Journal of Polymer Science)*, 2012, **30**, 1–15;

7 P. Thirumurugan, D. Matosiuk and K. Jozwiak, *Chem. Rev.*, 2013, **113**, 4905–4979.

8 C. Wentrup, *Tetrahedron*, 1970, **26**, 4969–4983.

9 A. Könnecke, R. Dörre, E. Kleinpeter and E. Lippmann, *Tetrahedron*, 1979, **35**, 1957–1963.

10 W. E. Hull, M. Künstlinger and E. Breitmaier, *Angew. Chem. Int. Ed. Engl.*, 1980, **19**, 924–926.

11 C. Temple and J. A. Montgomery, *J. Org. Chem.*, 1965, **30**, 826–829.

12 S. L. Deev, Z. O. Shenkarev, T. S. Shestakova, O. N. Chupakhin, V. L. Rusinov and A. S. Arseniev, *J. Org. Chem.*, 2010, **75**, 8487–8497.

13 C. Thétaz, F. W. Wehrli and C. Wentrup, *Helv. Chim. Acta*, 1976, **59**, 259–264.

14 I. A. Khalymbadzha, T. S. Shestakova, S. L. Deev, V. L. Rusinov, O. N. Chupakhin, Z. O. Shenkarev and A. S. Arseniev, *Russ. Chem. Bull.*, 2013, **62**, 521–528.

15 C. Temple, M. C. Thorpe, W. C. Coburn and J. A. Montgomery, *J. Org. Chem.*, 1966, **31**, 935–938.

16 J. A. Montgomery, K. Hewson, S. J. Clayton and H. J. Thomas, *J. Org. Chem.*, 1966, **31**, 2202–2210.

17 Q. Zhang, X. Wang, C. Cheng, R. Zhu, N. Liu and Y. Hu, *Org. Biomol. Chem.*, 2012, **10**, 2847–2854.

18 M. K. Lakshman, M. K. Singh, D. Parrish, R. Balachandran and B. W. Day, *J. Org. Chem.*, 2010, **75**, 2461–2473.

19 E. R. El-Sawy, M. S. Ebaid, H. M. Abo-Salem, A. G. Al-Sehemi and A. H. Mandour, *Arabian J. Chem.*, 2014, **7**, 914–923.

20 V. P. Krivopalov, E. B. Nikolaenkova, V. F. Sedova and V. P. Mamaev, *Chem. Heterocycl. Compd.*, 1983, **19**, 1116–1120.

21 V. P. Krivopalov, E. B. Nikolaenkova, V. F. Sedova and V. P. Mamaev, *Chem. Heterocycl. Compd.*, 1983, **19**, 977–981.

22 R. Huisgen, K. v. Fraunberg and H. J. Sturm, *Tetrahedron Lett.*, 1969, **10**, 2589–2594.

23 R. Sun, H. Wang, J. Hu, J. Zhao and H. Zhang, *Org. Biomol. Chem.*, 2014, **12**, 5954–5963.

24 L. Cosyn, K. K. Palaniappan, S.-K. Kim, H. T. Duong, Z.-G. Gao, K. A. Jacobson and S. van Calenbergh, *J. Med. Chem.*, 2006, **49**, 7373–7383.

25 B. Chattopadhyay, Vera, Claudia I Rivera, S. Chuprakov and V. Gevorgyan, *Org. Lett.*, 2010, **12**, 2166–2169.

26 A. M. Alanazi, A. A.-M. Abdel-Aziz, I. A. Al-Suwaidan, S. G. Abdel-Hamide, T. Z. Shawer and A. S. El-Azab, *Eur. J. Med. Chem.*, 2014, **79**, 446–454.

27 a) M. M. Ghorab, M. S. Alsaid, M. Ceruso, Y. M. Nissan and C. T. Supuran, *Bioorg. Med. Chem.*, 2014, **22**, 3684–3695; b) F. I. Hanafy, *Eur. J. Chem.*, 2011, **2**, 65–69; c) M. S. Mohamed, M. M. Youns and N. M. Ahmed, *Eur. J. Med. Chem.*, 2013, **69**, 591–600; d) S.-B. Wang, X.-Q. Deng, D.-C. Liu, H.-J. Zhang and Z.-S. Quan, *Med. Chem. Res.*, 2014, **23**, 4619–4626;

28 C. de Graaf, A. J. Kooistra, H. F. Vischer, V. Katritch, M. Kuijer, M. Shiroishi, S. Iwata, T. Shimamura, R. C. Stevens, de Esch, Iwan J P and R. Leurs, *J. Med. Chem.*, 2011, **54**, 8195–8206.

29 Zordok, Wael., A., *IJAST*, 2012, **2**, 339–357.

30 M. Kanyalkar and E. C. Coutinho, *Tetrahedron*, 2000, **56**, 8775–8777.

31 Majid Monajjemi, H. Bahareh and M. Hadieh, *J. Mex. Chem. Soc.*, 2006, **50**, 143–148.
32 A. Klamt and G. Schüürmann, *J. Chem. Soc., Perkin Trans. 2*, 1993, 799.
33 V. P. Krivopalov, V. I. Mamatyuk and E. B. Nikolaenkova, *Russ. Chem. Bull.*, 1995, **44**, 1435–1443.
34 a) A. Thomann, C. Börger, M. Empting and R. Hartmann, *Synlett*, 2014, **25**, 935–938; b) E. Weidel, M. Negri, M. Empting, S. Hinsberger and R. W. Hartmann, *Future Med. Chem.*, 2014, **6**, 2057–2072;
35 T. Wada, A. Mochizuki, S. Higashiya, H. Tsuruoka, S.-i. Kawahara, M. Ishikawa and M. Sekine, *Tetrahedron Lett.*, 2001, **42**, 9215–9219.
36 A. Masternak, B. Skalski and J. Milecki, *J. Label. Compd. Radiopharm.*, 2007, **50**, 43–46.
37 M. Empting, O. Avrutina, R. Meusinger, S. Fabritz, M. Reinwarth, M. Biesalski, S. Voigt, G. Buntkowsky and H. Kolmar, *Angew. Chem. Int. Ed.*, 2011, **50**, 5207–5211.
38 V. Y. Pochinok, L. F. Avramenko, P. S. Grigorenko and V. N. Skopenko, *Russ. Chem. Rev.*, 1975, **44**, 481–492.
39 C. Hansch, A. Leo and R. W. Taft, *Chem. Rev.*, 1991, **91**, 165–195.
40 A. Jansma, Q. Zhang, B. Li, Q. Ding, T. Uno, B. Bursulaya, Y. Liu, P. Furet, N. S. Gray and B. H. Geierstanger, *J. Med. Chem.*, 2007, **50**, 5875–5877.
41 J. J. Fox, D. van Praag, I. Wempen, I. L. Doerr, L. Cheong, J. E. Knoll, M. L. Eidinoff, A. Bendich and G. B. Brown, *J. Am. Chem. Soc.*, 1959, **81**, 178–187.
42 D. J. Brown, *Nature*, 1950, **165**, 1010.
43 P. Bultinck, H. de Winter, W. Langenaeker and J. P. Tollenaere, eds., *Computational medicinal chemistry for drug discovery*, Marcel Dekker, New York, 2004.
44 S. Grimme, M. Steinmetz and M. Korth, *J. Org. Chem.*, 2007, **72**, 2118–2126.
45 S. N. Pieniazek, F. R. Clemente and K. N. Houk, *Angew. Chem. Int. Ed.*, 2008, **47**, 7746–7749.
46 J. W. Gibbs, *Elementary principles in statistical mechanics. Developed with especial reference to the rational foundation of thermodynamics*, Ox Bow Press, Woodbridge, Conn., 1981.
47 H. C. Kolb, M. G. Finn and K. B. Sharpless, *Angew. Chem. Int. Ed.*, 2001, **40**, 2004–2021.
48 a) V. V. Rostovtsev, L. G. Green, V. V. Fokin and K. B. Sharpless, *Angew. Chem. Int. Ed.*, 2002, **41**, 2596–2599; b) C. W. Tornøe, C. Christensen and M. Meldal, *J. Org. Chem.*, 2002, **67**, 3057–3064;
49 A. Kalniņa, Ē. Bizdēna, G. Kiselovs, A. Mishnev and M. Turks, *Chem. Heterocycl. Comp.*, 2014, **49**, 1667–1673.
50 A. Kovaļovs, I. Novosjolova, Ē. Bizdēna, I. Bižāne, L. Skardziute, K. Kazlauskas, S. Jursenas and M. Turks, *Tetrahedron Lett.*, 2013, **54**, 850–853.
51 F. Blanco, I. Alkorta and J. Elguero, *Tetrahedron*, 2011, **67**, 8724–8730.
52 P. L. Golas, N. V. Tsarevsky and K. Matyjaszewski, *Macromol. Rapid Commun.*, 2008, **29**, 1167–1171.
53 E. M. Sletten and C. R. Bertozzi, *Angew. Chem. Int. Ed.*, 2009, **48**, 6974–6998.
54 H. Fittler, O. Avrutina, B. Glotzbach, M. Empting and H. Kolmar, *Org. Biomol. Chem.*, 2013, **11**, 1848–1857.
55 D. E. Scott, A. G. Coyne, S. A. Hudson and C. Abell, *Biochemistry*, 2012, **51**, 4990–5003.
56 C. W. Murray and M. L. Verdonk, *J. Comput. Aided. Mol. Des.*, 2002, **16**, 741–753.
57 A. L. Hopkins, C. R. Groom and A. Alex, *Drug Discovery Today*, 2004, **9**, 430–431.
58 C. Abad-Zapatero, *Expert Opin. Drug Discov.*, 2007, **2**, 469–488.
59 M. Congreve, R. Carr, C. Murray and H. Jhoti, *Drug Discovery Today*, 2003, **8**, 876–877.
60 R. Leonardi, Y.-M. Zhang, C. O. Rock and S. Jackowski, *Prog. Lipid Res.*, 2005, **44**, 125–153.
61 M. P. Storz, C. K. Maurer, C. Zimmer, N. Wagner, C. Brengel, de Jong, Johannes C, S. Lucas, M. Müsken, S. Häussler, A. Steinbach and R. W. Hartmann, *J. Am. Chem. Soc.*, 2012, **134**, 16143–16146.
62 C. E. Dulcey, V. Dekimpe, D.-A. Fauvelle, S. Milot, M.-C. Groleau, N. Doucet, L. G. Rahme, F. Lépine and E. Déziel, *Chem. Biol.*, 2013, **20**, 1481–1491.
63 M. D. Shultz, *Bioorg. Med. Chem. Lett.*, 2013, **23**, 5980–5991.
64 S. Schultes, C. de Graaf, E. E. Haaksma, de Esch, Iwan J.P., R. L. Leurs and O. Krämer, *Drug Discovery Today: Technol.*, 2010, **7**, e147-202.
65 F. H. Allen, C. M. Bird, R. S. Rowland and P. R. Raithby, *Acta Crystallogr. B Struct. Sci.*, 1997, **53**, 696–701.
66 A. L. Hopkins, G. M. Keserü, P. D. Leeson, D. C. Rees and C. H. Reynolds, *Nat. Rev. Drug Discovery*, 2014, **13**, 105–121.
67 P. N. Mortenson and C. W. Murray, *J. Comput. Aided. Mol. Des.*, 2011, **25**, 663–667.
68 J. A. Mindell, *Annu. Rev. Physiol.*, 2012, **74**, 69–86.
69 Y. Kato, S. Ozawa, C. Miyamoto, Y. Maehata, A. Suzuki, T. Maeda and Y. Baba, *Cancer Cell Int.*, 2013, **13**, 89.
70 D. E. Becker and K. L. Reed, *Anesth. Prog.*, 2006, **53**, 98–109.